Performance analysis of tabletop single-pulse terahertz detection at rates up to 1.1 MHz

Nicolas Couture,[1,2,†] Markus Lippl,[3,4] Wei Cui,[1,2] Angela Gamouras,[5,1] Nicolas Y. Joly,[4,3,6] and Jean-Michel Ménard[1,2,5,*]

[1] *Department of Physics, University of Ottawa, 25 Templeton Street, Ottawa, Ontario K1N 6N5, Canada*
[2] *Max Planck Centre for Extreme and Quantum Photonics, Ottawa, Ontario K1N 6N5, Canada*
[3] *Max Planck Institute for the Science of Light, 91058 Erlangen, Germany*
[4] *Department of Physics, University of Erlangen-Nürnberg, 91058 Erlangen, Germany*
[5] *National Research Council Canada, Ottawa, Ontario K1A 0R6, Canada*
[6] *Interdisciplinary Center for Nanostructured Films, 91058 Erlangen, Germany*

(Received 3 January 2024; revised 15 March 2024; accepted 12 April 2024; published 9 May 2024)

Standard terahertz time-domain spectroscopy uses a relatively slow multidata acquisition process that has hindered the technique's ability to resolve "fast" dynamics occurring on the microsecond timescale. This timescale, inaccessible to most ultrafast pump-probe techniques, hosts a range of phenomena that has been left unexplored due to a lack of proper real-time monitoring techniques. In this work, chirped-pulse spectral encoding, a photonic time-stretch technique, and high-speed electronics are used to demonstrate time-resolved terahertz detection at a rate up to 1.1 MHz. This configuration relies on a tabletop optical source and a setup able to resolve every terahertz transient generated by the same source. We investigate the performance of this single-pulse terahertz detection system at different acquisition rates in terms of experimental noise, dynamic range, and signal-to-noise ratio. Our results pave the way towards single-pulse terahertz time-domain spectroscopy at arbitrarily fast rates to monitor complex dynamics in real time.

DOI: 10.1103/PhysRevApplied.21.054020

I. INTRODUCTION

Terahertz time-domain spectroscopy (TDS) relies on resolving the oscillating electric field of a terahertz pulse in order to access its frequency components via Fourier transform. This technique provides full amplitude and phase information on the light passing through a medium, allowing the complex dielectric function of the medium to be extracted without the need for Kramers-Kronig relations, a powerful capability compared with other spectroscopic techniques monitoring only the transmitted optical power. Terahertz TDS is often performed with a detection technique involving the mechanical scanning of an ultrashort near-infrared (NIR) pulse across the terahertz waveform as the two interact in a nonlinear crystal. Because this technique intrinsically relies on the acquisition of multiple data points to reconstruct the full terahertz waveform, it requires the sample under study to exhibit the same characteristics every time it is probed by the terahertz wave. Thus, the standard pump-probe technique is not viable in evaluating samples whose properties evolve chaotically or experience irreversible changes. Many studies have tackled this issue by enabling single-shot terahertz detection, eliminating the need for a mechanical delay line to retrieve the time-domain terahertz waveform. These techniques, however, require data averaging to reach a sufficiently high signal-to-noise ratio (SNR) to extract relevant information. These systems, collecting data at kilohertz rates [1], often rely on a detection scheme using echelon mirrors [2], chirped-pulse spectral encoding [3], or spectral interferometry [4]. Operation at megahertz rates has also been demonstrated with a combination of chirped-pulse spectral encoding and a photonic time-stretch technique [5,6], where the repetition rate of the NIR source used for spectral encoding sets the acquisition rate [7–10]. However, these single-pulse megahertz-rate experiments were achieved with high-energy terahertz pulses from synchrotron facilities to achieve a satisfactory SNR. To perform spectroscopic studies of materials, synchrotron facilities are not as easily accessible and practical as tabletop terahertz sources, which also generally offer a more stable output. Recently, single-pulse terahertz TDS at a rate of 50 kHz with an ultrafast source was used to resolve pulse-to-pulse microsecond carrier dynamics in a

*Corresponding author: jean-michel.menard@uottawa.ca
†Current address: National Research Council Canada, 100 Sussex Drive, Ottawa, Ontario K1A 0R6, Canada.

semiconductor [11]. Reaching faster terahertz-TDS rates with tabletop sources would allow complex dynamics at submicrosecond timescales to be recorded and would significantly expedite the data-acquisition process in some experiments, such as those involving terahertz two-dimensional spectroscopy [12]. In this work, we present a quantitative study on the noise limitations of a tabletop single-pulse terahertz-TDS system. The single-pulse detection technique uses chirped-pulse spectral encoding and a photonic time-stretch technique operated at a rate up to 1.1 MHz, the fastest rate achieved to resolve terahertz waveforms with a single tabletop optical source. We characterize the system through its dynamic range and SNR, which are crucial parameters in establishing the suitability of the technique for practical spectroscopy purposes. With standard terahertz detection techniques, these parameters can be extracted by well-known methods [13], and they depend on the measurement integration time [14]. Since single-pulse data acquisition intrinsically cannot rely on time averaging, a benchmark must be established to evaluate the performance of single-pulse terahertz systems. Here we propose such an approach and present measurements that can serve as references for future work on single-pulse spectroscopy. Interestingly, when terahertz transients are recorded as frequently as every 5 μs, we still measure a spectral dynamic range (more than 30 dB in power) and SNR (approximately 25) that is sufficient to enable a range of spectroscopic applications. This sensitive detection regime is, however, achieved only when we avoid using a noisy spectral region of the supercontinuum (SC) gating pulse, which is located around the wavelength of the excitation NIR pulse. Our results lay the foundation for tabletop terahertz TDS at high acquisition rates as a real-time monitoring tool with submicrosecond resolution [15].

II. EXPERIMENT

For these experiments, an amplified ultrafast source centered at a wavelength of 1030 nm delivers 180-fs pulses for terahertz generation and detection. The laser is operated at its maximum average power of 6 W and its repetition rate is modified via software between 1 kHz and 1.1 MHz, with only the output peak intensity altered, while chirp and pulse duration remain effectively unaffected. Most of the output power (90%) is used for terahertz generation via optical rectification in a lithium niobate crystal with the tilted-pulse-front technique [16]. The terahertz pulse is guided by a series of off-axis parabolic mirrors and focused by one of these mirrors (NA approximately 0.5) to achieve a relatively tight terahertz focal spot of approximately 500 μm ($1/e^2$). The rest of the beam is set to a constant pulse energy of approximately 10 nJ and launched into a 2-m-long polarization-maintaining fiber (PMF; OZ Optics PMF-980-6/125-0.25-L) to generate a chirped NIR SC spanning approximately 100 nm with a duration of 6 ps (FWHM) for each of the explored repetition rates. Low NIR-pulse energies were used to ensure SC stability and to considerably reduce the risk of thermal damage over long periods of laser exposure. A chirped SC with these specifications allows frequencies up to 1.6 THz to be detected through chirped-pulse spectral encoding, imprinting the time-domain terahertz waveform onto the chirped NIR spectrum through nonlinear effects [3,11]. Here we achieve chirped-pulse spectral encoding by overlapping the resulting terahertz pulse and chirped SC in a 2-mm-thick (110)-oriented gallium phosphide (GaP) crystal, a material with favorable phase-matching conditions, featuring a coherence length exceeding 3.5 mm, for excitation wavelengths near 1 μm and terahertz frequencies below 2 THz. The NIR pulse containing the terahertz information is transmitted through a quarter-wave plate and linear polarizer to optimize detection sensitivity while maintaining the phase information of the terahertz pulse [17]. Finally, the encoded NIR pulse is launched into a 2-km-long single-mode fiber (SMF; Corning HI1060 flex) to achieve photonic time stretch, dispersing the pulse duration from a few picoseconds to tens of nanoseconds, which can then be sampled with a high-speed photodiode (12-GHz bandwidth, Newport 1544-B) and oscilloscope (8-GHz bandwidth, Tektronix MSO64B). A diagram of the experimental configuration is shown in Fig. 1. With

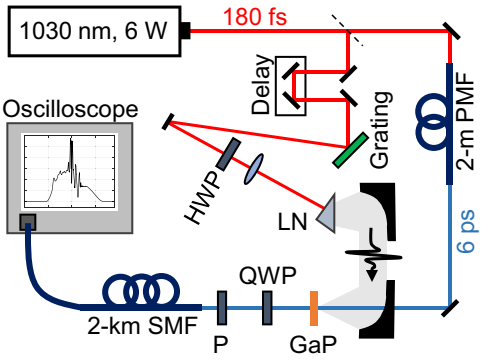

FIG. 1. Experimental setup. A Yb:KGW amplifier with average power of 6 W and a tunable repetition rate is used for terahertz generation and detection. Most of the optical power is used for terahertz generation with a tilted-pulse-front technique in a lithium niobate (LN) crystal wedge. The remainder is launched into a 2-m-long PMF to generate a chirped SC with 100-nm bandwidth and 6-ps duration (FWHM). The terahertz pulse and the chirped SC are overlapped in a 2-mm-thick GaP crystal to achieve chirped-pulse spectral encoding, imprinting the terahertz waveform onto the chirped NIR spectrum through the Pockels effect. After polarization filtering with a quarter-wave plate (QWP) and a linear polarizer (P), photonic time stretch is realized by our injecting the terahertz-modulated SC into a 2-km-long SMF and detecting it with a fast photodiode (12 GHz) and oscilloscope (8 GHz). HWP, half-wave plate.

this technique, the terahertz detection rate can be arbitrarily high and is determined solely by the repetition rate of the ultrafast source providing NIR-pulse energies of at least a few microjoules. Our single-pulse terahertz detection technique, based on electro-optic sampling, has a detection sensitivity limited mainly by the nonlinear conversion efficiency in the terahertz detection crystal. This efficiency could potentially be increased, notably by one (i) using a more-powerful NIR source to achieve higher terahertz-pulse energies, (ii) relying on a detection crystal with a larger second-order nonlinearity, while still ensuring a long nonlinear interaction length, or (iii) ensuring a tighter terahertz focusing on the detection crystal.

III. RESULTS AND DISCUSSION

To retrieve the terahertz waveform through the photonic time-stretch technique, the signal is recorded on the oscilloscope with and without the terahertz pulse impinging on the GaP crystal, as shown in Fig. 2(a) (red line and dashed black line, respectively). Subtraction of the square root of each measurement yields the terahertz waveform in the time-stretch domain [11]. The recovered waveform is presented in Fig. 2(b) when the delay between the chirped SC and the terahertz pulse is varied in increments of 500 fs. By our imprinting the terahertz waveform on a different portion of the NIR spectrum, the time axis of the oscilloscope can be calibrated to retrieve the picosecond information for the terahertz pulse. The linear relationship between the terahertz peak measured on the oscilloscope and the relative delay allows us to extract a time-stretch factor of 1138 and confirms that higher-order dispersion in the 2-km-long SMF is negligible [5]. The input NIR-pulse energy injected into the PMF is set at 10 nJ to optimize pulse-to-pulse stability. This ensures a stable SC spectral width and corresponding time-stretch factor, which is experimentally verified.

The shaded gray areas in Fig. 2 correspond to the portion of the spectrum where the terahertz waveforms are subject to deformations, and that we have therefore deemed suboptimal for spectral encoding. This spectral region, near the pump wavelength, is dominated by characteristic sharp ripples of self-phase modulation, which are extremely sensitive to minor fiber-coupling fluctuations, while optical wave breaking smooths out the rest of spectrum [18]. The flat portions of the spectrum do not possess this fiber-coupling sensitivity and therefore have lower noise, except at the extreme edges of the spectrum [Fig. 2(c)]. Delaying the pulses such that the terahertz waveform is imprinted on the most stable parts of the NIR spectrum is a valid method of performing these experiments as the terahertz information is contained within only approximately 4 ns and the time-stretched spectrum spans more than 20 ns. It is crucial to imprint the terahertz data within a region of the SC where phase-matching conditions are constant for

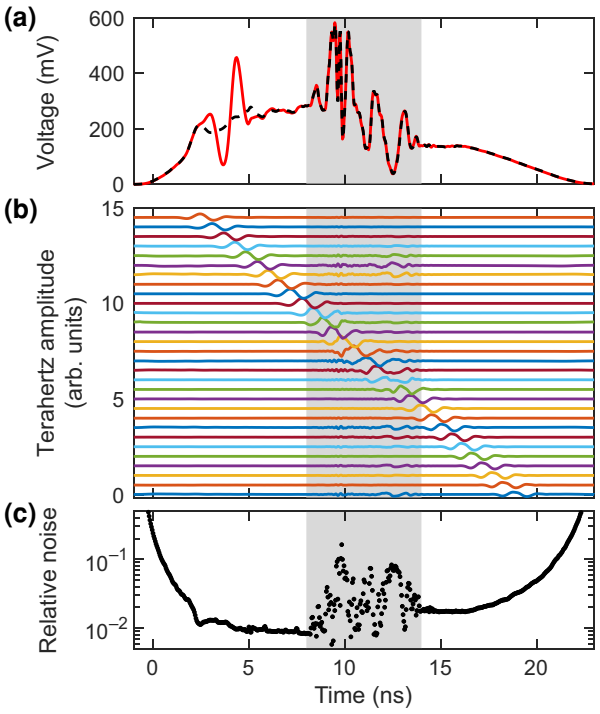

FIG. 2. Time-axis calibration. (a) Unmodulated (dashed black line) and terahertz-modulated (red line) time-stretched signals measured with the fast photodiode and oscilloscope. To isolate the terahertz waveform, the square root of the unmodulated signal is subtracted from the square root of the terahertz-modulated signal. (b) Extracted terahertz waveforms as the relative delay between the terahertz pulse and the chirped SC is shifted in increments of 500 fs, varying the frequencies within the SC onto which the terahertz transient is imprinted. The waveforms are stacked vertically for clarity. The shaded gray area indicates noisy parts of the spectrum and is quantified by (c) the relative noise of the SC, which we define as the standard deviation of the SC signal (voltage on the oscilloscope) divided by the mean SC signal.

all NIR spectral components, which are effectively acting as independent gating pulses. In our experiment, this condition is satisfied for terahertz frequencies between 0.5 and 1.5 THz since it relies on a GaP detection crystal and a NIR spectral window between 970 and 1010 nm [19]. However, a reliable decoding of a terahertz waveform overlapping with the full SC, which extends from 960 to 1080 nm, would require the development of a transfer function that considers the variations in phase-matching conditions.

The noise recorded in these most stable regions is dominated by electronic noise from the oscilloscope, photodiode, power supply, or any combination thereof, with only minor contributions from pulse-to-pulse laser power fluctuations. The standard deviation of the total SC spectral power, corresponding to a pulse energy of approximately 6 nJ incident on the GaP crystal, is less than 1%. To use the

entire SC spectrum for spectral encoding, balanced detection techniques adapted to single-pulse detection, such as diversity electro-optic sampling [20,21], can be used to reduce pulse-to-pulse fluctuations but will not help if the main source of noise is electronic.

Figure 3(a) displays the extracted time-domain terahertz waveform after the time-axis calibration has been performed for laser output pulse energies of 120, 20, and 5.5 μJ, corresponding to laser repetition rates of 50 kHz, 300 kHz, and 1.1 MHz, respectively. The field strength and pulse energy of the terahertz pulses, in kilovolts per centimeter and picojoules, are extracted with electro-optic sampling and not the single-pulse detection configuration [22]. For clarity, the data in Fig. 3(a) collected with NIR-pulse energies 20 and 5.5 μJ are multiplied by factors of 3 and 4, respectively. The shaded areas surrounding the colored lines in Fig. 3(a) represent the standard deviation measured over 10 000 pulses. Although the signal at 5.5 μJ (1.1 MHz) is weaker, this result marks, to our knowledge, the fastest tabletop time-resolved terahertz detection rate to date.

The terahertz waveform is measured for several pulse energies to form the line plotted in Fig. 3(b), where the peak terahertz amplitude and corresponding pulse energy inside the GaP crystal are shown as a function of the laser output pulse energy. The linear relationship between the NIR-pulse energy and the detected terahertz amplitude validates the linearity of the polarization filtering scheme in Fig. 1 [11]. For each measurement, the pulse energy injected into the PMF is kept fixed at approximately 10 nJ; hence, the NIR-pulse energy in the GaP detection crystal is also fixed, indicating that the detection efficiency is not limited by the repetition rate but instead is limited by the terahertz-field strength inside the crystal. The highest terahertz field in this work, corresponding to the red line in Fig. 3(a), is approximately 35 kV/cm and corresponds to a terahertz-pulse energy of approximately 85 pJ. This value, comparable to those obtained by other groups using similar terahertz sources [23], partly determines the sensitivity of the single-pulse terahertz spectrometer. In contrast to other schemes, since our system relies on only a single laser and a single photodiode, timing jitter is negligible. Jitter between the terahertz pulse and the SC would appear in the experimental data as phase noise. In this work, the standard deviation of the phase is on the order of 10^{-2} rad across the whole spectrum. This feature makes it highly suitable as a noninvasive probe in industrial assembly lines. The temporal shift between the terahertz pulse and the SC induced by a product in the path of the terahertz beam can be used to extract the thickness of the product with great accuracy.

For a more-in-depth analysis of the measured terahertz waveforms at each of the repetition rates studied, we calculate the dynamic range of the recorded time-domain signals [Fig. 4(a)] and their corresponding spectral amplitude [Fig. 4(b)]. To optimize the SNR of our

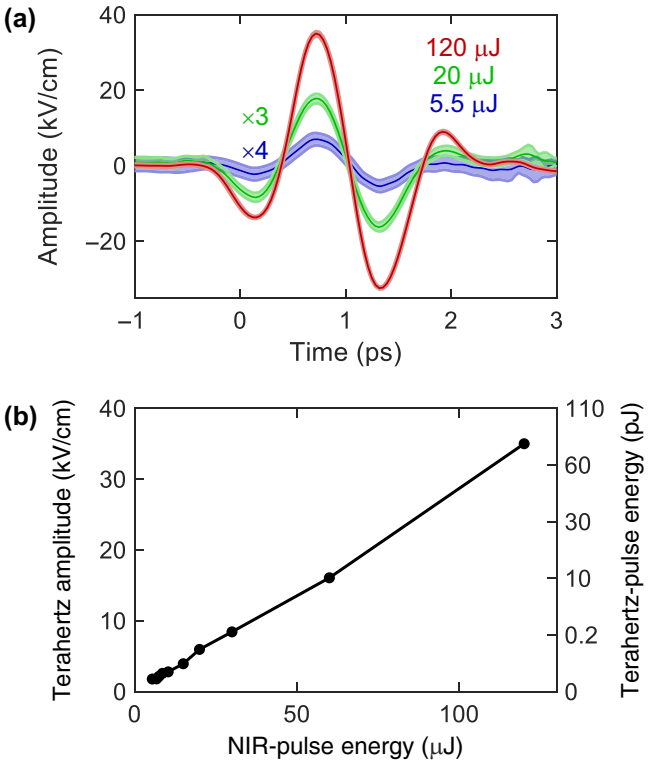

FIG. 3. Relative-amplitude characterization. (a) Extracted terahertz transients generated with NIR-pulse energies of 120 μJ (red), 20 μJ (green), and 5.5 μJ (blue); corresponding to detection rates of 50 kHz, 300 kHz, and 1.1 MHz, respectively. The solid lines represent the averaged waveforms and the shaded areas represent the error of the measurement calculated from the standard deviation over 10 000 pulses. For clarity, the blue and green lines (and their corresponding standard deviation) are multiplied by factors of 3 and 4, respectively. (b) Peak terahertz-transient amplitude inside the GaP crystal as the pulse energy of the ultrafast source is increased from 5.5 to 120 μJ by decreasing the repetition rate (i.e., 1.1 MHz to 50 kHz). The linear relationship between the detected terahertz amplitude and the NIR-pulse energy indicates that the system can reach higher detection rates at the cost of detection efficiency. The highest terahertz field, corresponding to a detection rate of 50 kHz, is approximately 35 kV/cm or approximately 85 pJ.

detected terahertz spectrum, we perform a Fourier transform of the time-resolved terahertz waveform within a 4-ps window, which avoids the noisier NIR region located around the excitation wavelength (shaded gray region in Fig. 2). The width of this time window is inversely proportional to the smallest spectral interval one can resolve with this technique. To increase the spectral resolution, it might be possible to use an all-normal dispersion optical fiber to generate an extremely broadband and low-noise SC [24]. The choice of terahertz detection crystal also has a direct impact on the accessible spectral bandwidth. Because of phase-matching conditions, a thick crystal provides access to a limited spectral region, while a thinner crystal can be

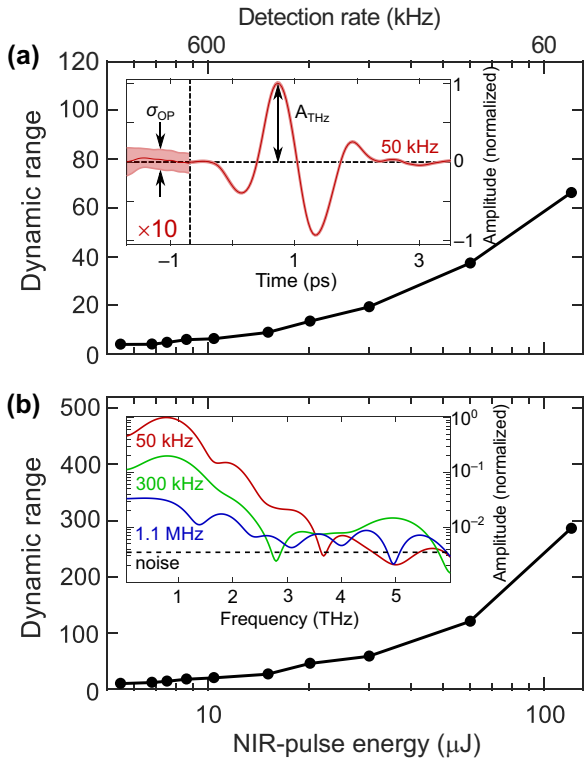

FIG. 4. Dynamic range of single-pulse terahertz detection. The dynamic range of the presented scheme as a function of (a) the detection rate and (b) the NIR-pulse energy. The dynamic ranges of (a) the recorded time-domain data and (b) corresponding terahertz spectra are calculated with the methods described in Ref. [13]. The arrows in the inset in (a) indicate parts of the terahertz waveform used to calculate the dynamic range. The inset in (b) contains terahertz spectra (plotted on a logarithmic scale) recorded at repetition rates of 50 kHz (red), 300 kHz (green), 1.1 MHz (blue) and the noise floor of the single-pulse case (dashed black line).

used to resolve a larger bandwidth, although at the expense of lower detection sensitivity [25,26]. The dynamic range in the time domain is defined as the mean of the peak terahertz amplitude (A_{THz}) divided by the off-peak standard deviation (σ_{OP}), whereas in the Fourier domain it is defined as the maximum spectral amplitude of a single-pulse measurement divided by the noise floor [dashed black line in the inset in Fig. 4(b)] [13]. Notably, the peak dynamic range approaches 300 in amplitude (50 dB in power) in the Fourier domain when the system is operated at 50 kHz. The SNR of the single-pulse data can be extracted with a similar approach. In both domains, the SNR is defined as the quotient between the peak terahertz amplitude and the on-peak standard deviation [13]. The peak SNR achieved with a repetition rate of 50 kHz is approximately 60 in the time domain and approximately 150 in the Fourier domain. The dynamic range in each case follows the same trend: as the repetition rate is increased, the dynamic range decreases correspondingly. This trend is a result of the weaker nonlinear interactions in the GaP detection crystal and the constant noise floor. At repetition rates exceeding 600 kHz, the frequency-domain SNR of the single-pulse measurement can be considered too low to obtain clear spectroscopic information without pulse-to-pulse averaging. Nonetheless, in the time domain, amplitude changes and temporal shifts of the terahertz pulse can still be monitored to investigate different phenomena. Our analysis is obtained in the absence of a sample in the path of the terahertz beam, which is a common practice to characterize new photonics systems [13,14]. Sample absorption and Fresnel reflections should therefore be considered when one is evaluating the feasibility of experiments at high repetition rates, although many samples, including polymers and molecular gases, should not considerably affect the values reported in Fig. 4.

IV. CONCLUSION

In summary, we have used chirped-pulse spectral encoding and a photonic time-stretch technique to demonstrate time-resolved terahertz detection at a rate up to 1.1 MHz using a single ultrafast source, to our knowledge the fastest tabletop single-pulse detection rate to date. By thoroughly investigating the noise of the presented system, we have deduced the limitation of the system to be the terahertz-field strength at high repetition rates and, hence, low NIR-pulse energies. With the simple addition of high-speed electronics and commercially available optical fibers, existing systems with high terahertz fields (tens of kilovolts per centimeter) can almost effortlessly implement the presented detection scheme. Finally, considering potential technical improvements that can still be implemented in the setup, especially regarding the reduction of electronic noise and the increase of the terahertz generation and detection efficiencies, we foresee this technique could be routinely used with an oscillator source operating at 100 MHz to perform real-time single-pulse terahertz monitoring of nanosecond dynamics and explore a range of new phenomena.

ACKNOWLEDGMENTS

J.-M.M. acknowledges funding from the Natural Sciences and Engineering Research Council of Canada (Grants No. RGPIN-2023-05365 and No. RTI-2023-00252) and the Canada Foundation for Innovation (Project No. 35269). N.C. acknowledges financial support from the Ontario Graduate Scholarship. M.L. is a member of the Max Planck School of Photonics supported by BMBF, the Max Planck Society, and the Fraunhofer Society. N.Y.J. and M.L. acknowledge the Max Planck – uOttawa Centre for Extreme and Quantum Photonics for financial support. This work was also supported by the National Research Council of Canada via the Joint Centre for Extreme Photonics.

[1] S. M. Teo, B. K. Ofori-Okai, C. A. Werley, and K. A. Nelson, Invited Article: Single-shot THz detection techniques optimized for multidimensional THz spectroscopy, Rev. Sci. Instrum. **86**, 051301 (2015).

[2] Y. Minami, Y. Hayashi, J. Takeda, and I. Katayama, Single-shot measurement of a terahertz electric-field waveform using a reflective echelon mirror, Appl. Phys. Lett. **103**, 051103 (2013).

[3] Z. Jiang and X.-C. Zhang, Electro-optic measurement of THz field pulses with a chirped optical beam, Appl. Phys. Lett. **72**, 1945 (1998).

[4] G. Sharma, K. Singh, I. Al-Naib, R. Morandotti, and T. Ozaki, Terahertz detection using spectral domain interferometry, Opt. Lett. **37**, 4338 (2012).

[5] K. Goda, D. R. Solli, K. K. Tsia, and B. Jalali, Theory of amplified dispersive Fourier transformation, Phys. Rev. A **80**, 043821 (2009).

[6] K. Goda and B. Jalali, Dispersive Fourier transformation for fast continuous single-shot measurements, Nat. Photonics **7**, 102 (2013).

[7] E. Roussel, C. Evain, M. Le Parquier, C. Szwaj, S. Bielawski, L. Manceron, J.-B. Brubach, M.-A. Tordeux, J.-P. Ricaud, L. Cassinari, M. Labat, M.-E. Couprie, and P. Roy, Observing microscopic structures of a relativistic object using a time-stretch strategy, Sci. Rep. **5**, 10330 (2015).

[8] C. Szwaj, C. Evain, M. Le Parquier, P. Roy, L. Manceron, J.-B. Brubach, M.-A. Tordeux, and S. Bielawski, High sensitivity photonic time-stretch electro-optic sampling of terahertz pulses, Rev. Sci. Instrum. **87**, 103111 (2016).

[9] C. Evain, E. Roussel, M. Le Parquier, C. Szwaj, M.-A. Tordeux, J.-B. Brubach, L. Manceron, P. Roy, and S. Bielawski, Direct observation of spatiotemporal dynamics of short electron bunches in storage rings, Phys. Rev. Lett. **118**, 054801 (2017).

[10] B. Steffen, C. Gerth, M. Caselle, M. Felber, T. Kozak, D. R. Makowski, U. Mavrič, A. Mielczarek, P. Peier, K. Przygoda, and L. Rota, Compact single-shot electro-optic detection system for THz pulses with femtosecond time resolution at MHz repetition rates, Rev. Sci. Instrum. **91**, 045123 (2020).

[11] N. Couture, W. Cui, M. Lippl, R. Ostic, D. J. J. Fandio, E. K. Yalavarthi, A. Vishnuradhan, A. Gamouras, N. Y. Joly, and J.-M. Ménard, Single-pulse terahertz spectroscopy monitoring sub-millisecond time dynamics at a rate of 50 kHz, Nat. Commun. **14**, 2595 (2023).

[12] F. Y. Gao, Z. Zhang, Z.-J. Liu, and K. A. Nelson, High-speed two-dimensional terahertz spectroscopy with echelon-based shot-to-shot balanced detection, Opt. Lett. **47**, 3479 (2022).

[13] M. Naftaly and R. Dudley, Methodologies for determining the dynamic ranges and signal-to-noise ratios of terahertz time-domain spectrometers, Opt. Lett. **34**, 1213 (2009).

[14] J. Neu and C. A. Schmuttenmaer, Tutorial: An introduction to terahertz time domain spectroscopy (THz-TDS), J. Appl. Phys. **124**, 231101 (2018).

[15] A. Mahjoubfar, D. V. Churkin, S. Barland, N. Broderick, S. K. Turitsyn, and B. Jalali, Time stretch and its applications, Nat. Photonics **11**, 341 (2017).

[16] J. Hebling, K.-L. Yeh, M. C. Hoffmann, B. Bartal, and K. A. Nelson, Generation of high-power terahertz pulses by tilted-pulse-front excitation and their application possibilities, J. Opt. Soc. Am. B **25**, B6 (2008).

[17] Z. Jiang, F. G. Sun, Q. Chen, and X.-C. Zhang, Electro-optic sampling near zero optical transmission point, Appl. Phys. Lett. **74**, 1191 (1999).

[18] A. M. Heidt, Pulse preserving flat-top supercontinuum generation in all-normal dispersion photonic crystal fibers, J. Opt. Soc. Am. B **27**, 550 (2010).

[19] Q. Wu and X.-C. Zhang, 7 terahertz broadband GaP electro-optic sensor, Appl. Phys. Lett. **70**, 1784 (1997).

[20] E. Roussel, C. Szwaj, C. Evain, B. Steffen, C. Gerth, B. Jalali, and S. Bielawski, Phase diversity electro-optic sampling: A new approach to single-shot terahertz waveform recording, Light Sci. Appl. **11**, 14 (2022).

[21] E. Roussel, C. Szwaj, P. D. Pietro, N. Adhlakha, P. Cinquegrana, M. Veronese, C. Evain, S. D. Mitri, A. Perucchi, and S. Bielawski, Single-shot terahertz time-domain spectrometer using 1550 nm probe pulses and diversity electro-optic sampling, Opt. Express **31**, 31072 (2023).

[22] F. Blanchard, L. Razzari, H.-C. Bandulet, G. Sharma, R. Morandotti, J.-C. Kieffer, T. Ozaki, M. Reid, H. F. Tiedje, H. K. Haugen, and F. A. Hegmann, Generation of 1.5 uJ single-cycle terahertz pulses by optical rectification from a large aperture ZnTe crystal, Opt. Express **15**, 13212 (2007).

[23] P. L. Kramer, M. K. R. Windeler, K. Mecseki, E. G. Champenois, M. C. Hoffmann, and F. Tavella, Enabling high repetition rate nonlinear THz science with a kilowatt-class sub-100 fs laser source, Opt. Express **28**, 16951 (2020).

[24] M. Lippl, M. H. Frosz, and N. Y. Joly, Low-noise supercontinuum generation in chiral all-normal dispersion photonic crystal fibers, Opt. Lett. **48**, 5297 (2023).

[25] A. Halpin, W. Cui, A. W. Schiff-Kearn, K. M. Awan, K. Dolgaleva, and J.-M. Ménard, Enhanced terahertz detection efficiency via grating-assisted noncollinear electro-optic sampling, Phys. Rev. Appl. **12**, 031003 (2019).

[26] W. Cui, K. M. Awan, R. Huber, K. Dolgaleva, and J.-M. Ménard, Broadband and high-sensitivity time-resolved THz system using grating-assisted tilted-pulse-front phase matching, Adv. Opt. Mater. **10**, 2101136 (2022).